Journal of Medicinal Chemistry

Article

pubs.acs.org/jmc

Achiral Pyrazinone-Based Inhibitors of the Hepatitis C Virus NS3 Protease and Drug-Resistant Variants with Elongated Substituents Directed Toward the S2 Pocket

Johan Gising,[†,#] Anna Karin Belfrage,[†,#] Hiba Alogheli,[†] Angelica Ehrenberg,[‡] Eva Åkerblom,[†] Richard Svensson,[§,∥] Per Artursson,[§,∥] Anders Karlén,[†] U. Helena Danielson,[‡] Mats Larhed,[†] and Anja Sandström*[,†]

[†]Department of Medicinal Chemistry, Organic Pharmaceutical Chemistry, BMC, Uppsala University, Box 574, SE-751 23 Uppsala, Sweden

[‡]Department of Chemistry, BMC, Uppsala University, BMC, Box 576, SE-751 23 Uppsala, Sweden

[§]Department of Pharmacy, Uppsala University, Box 580, SE-751 23 Uppsala, Sweden

[∥]The Uppsala University Drug Optimization and Pharmaceutical Profiling Platform, Chemical Biology Consortium Sweden (CBCS), Uppsala University, Box 580, SE-751 23 Uppsala, Sweden

Supporting Information

ABSTRACT: Herein we describe the design, synthesis, inhibitory potency, and pharmacokinetic properties of a novel class of achiral peptidomimetic HCV NS3 protease inhibitors. The compounds are based on a dipeptidomimetic pyrazinone glycine P3P2 building block in combination with an aromatic acyl sulfonamide in the P1P1′ position. Structure−activity relationship data and molecular modeling support occupancy of the S2 pocket from elongated R^6 substituents on the 2(1*H*)-pyrazinone core and several inhibitors with improved inhibitory potency down to K_i = 0.11 μM were identified. A major goal with the design was to produce inhibitors structurally dissimilar to the di- and tripeptide-based HCV protease inhibitors in advanced stages of development for which cross-resistance might be an issue. Therefore, the retained and improved inhibitory potency against the drug-resistant variants A156T, D168V, and R155K further strengthen the potential of this class of inhibitors. A number of the inhibitors were tested in in vitro preclinical profiling assays to evaluate their apparent pharmacokinetic properties. The various R^6 substituents were found to have a major influence on solubility, metabolic stability, and cell permeability.

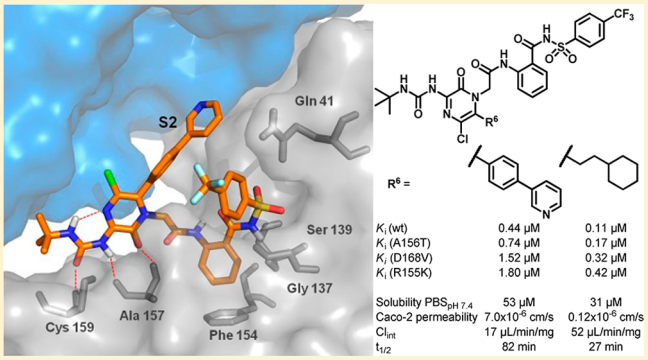

INTRODUCTION

Hepatitis C virus (HCV) is a widespread disease affecting approximately 130−200 million people worldwide.[1] Each year, 3−4 million people are newly infected and more than 350000 people die from HCV related liver diseases yearly.[1,2] Despite significant effort in the area, there is still no vaccine available.[3] About 70% of all infections will develop into a chronic HCV infection, which in one-fourth of the cases leads to cirrhosis and ultimately hepatocellular carcinoma or end-stage liver disease.[4] The standard treatment has long consisted of a combination therapy of pegylated interferon-α, which boosts the patient's immune system, and ribavirin, which inhibits the virus RNA replication (pegIFNα/RBV). The efficacy has been highly dependent on the genotype of the virus. Among individuals infected with HCV genotypes 1 or 4 less than 50% obtain a sustained virological response (SVR), whereas 85% of patients infected with genotypes 2 or 3 obtain SVR.[4,5] Furthermore, this treatment is associated with severe adverse effects and inconvenient dosing regimens.[4,5]

As an alternative or a complement to pegIFNα/RBV, direct acting antivirals (DAA), especially those targeting the NS3 protease, the NS5B polymerase, and the NS5A protein, which are all part of the replication complex, have been intensively explored as promising future drugs. Several DAAs are currently in the final stage of clinical development,[4] and the reversible covalent peptidomimetic NS3 protease inhibitors **1** (Telaprevir)[6] and **2** (Boceprevir)[7] were recently approved for the treatment of chronic HCV infection. These drugs (**1** or **2**) are now included in the standard therapy, in combination with pegIFNα/RBV (Figure 1), for people infected with genotype 1.[4−6] Besides positive qualities in terms of more efficient

Special Issue: HCV Therapies

Received: December 21, 2012
Published: March 21, 2013

   dx.doi.org/10.1021/jm301887f | *J. Med. Chem.* 2014, 57, 1790−1801

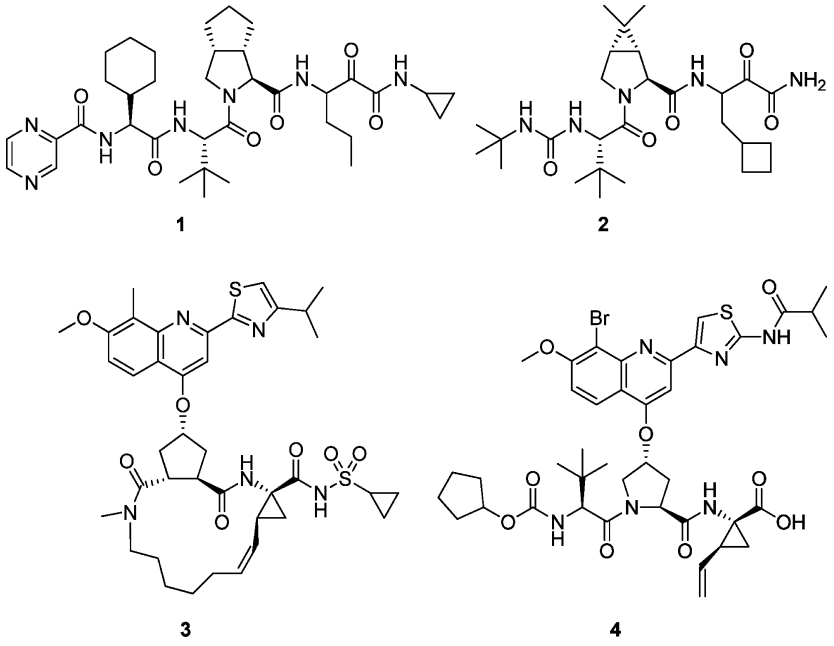

Figure 1. Direct acting antivirals of the hepatitis C virus NS3 protease. Telaprevir (**1**) and Boceprevir (**2**), approved covalent reversible inhibitors. Simeprevir/TMC435350 (**3**) and Faldaprevir/BI201335 (**4**), examples of clinically evaluated, noncovalent product-based inhibitors.

outcome and shorter treatment periods, both of these drugs are accompanied with a high pill burden and side effects, like rash and anemia, in addition to those caused by pegIFNα/RBV. Among the HCV NS3 protease inhibitors under clinical investigation, the most advanced are **3** (Simeprevir/TMC435350),[8] a noncovalent, macrocyclic inhibitor, and **4** (Faldaprevir/BI201335),[9] a noncovalent linear inhibitor (Figure 1). Both of the compounds are currently in phase 3 clinical studies. These promising drug candidates are dosed once daily instead of three times daily as required for **1** or **2** and are associated with fewer side effects.[10]

One major concern in HCV therapy, and especially in cases of low compliance, is potential development of drug resistance. This is a consequence of the high replication rate and the error-prone nature of the HCV RNA-dependent RNA polymerase.[11] Indeed, drug resistance has been observed frequently in in vivo and in vitro studies during treatment with **1** and **2** and several of the HCV NS3 protease inhibitors in advanced clinical development.[12,13] Critically, several of the amino acid substitutions observed in NS3 (i.e., A156T, D168V, and R155K etc.) convey some cross-resistance because the structures of **1**, **2**, and advanced drug candidates are somewhat similar; often based on a P2 proline/proline mimic.[10,12,14−17] To combat potential future problems with drug resistance, beside the obvious use of a combination therapy, there is a need for novel protease inhibitors based on unique structural motifs.

Aiming at new types of HCV NS3 protease inhibitors, we have previously explored macrocyclic and linear inhibitors based on P2 phenylglycine[18−20] and preliminary efforts to include a P3 2(1*H*)-pyrazinone scaffold (Figure 2).[21] The 2(1*H*)-pyrazinone scaffold possesses structural features useful in peptidomimetic compounds due to its ability to act as a β-strand inducer and retain the H-bonding pattern of the peptide backbone (Figure 2, I).[22,23] Compound **5** displayed single digit μM inhibitory potency against the full-length wild-type NS3 protease as well as promising activity against the resistant NS3 variants A156T and D168A (Figure 2), prompting further exploration of this class of inhibitors.[21] Preliminary results

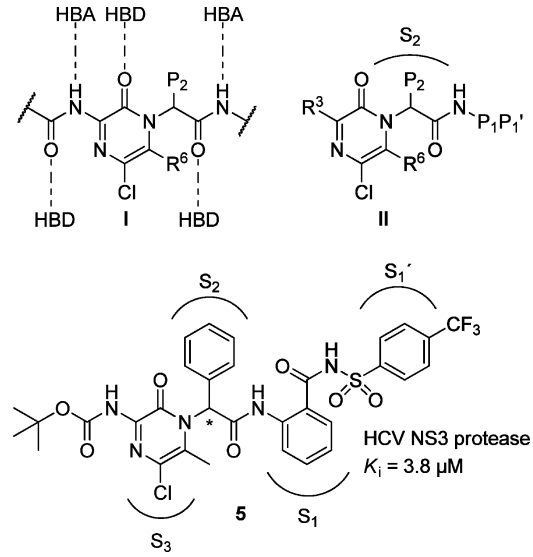

Figure 2. (I) Possible hydrogen bond interactions of the peptide backbone. (II) A schematic representation of the substituents on the pyrazinone scaffold. **5**, Pyrazinone comprising inhibitor.[21]

indicated that the large, not fully occupied, S2 pocket could be reached from the R^6 position of the pyrazinone (Figure 2, II).[21]

We herein demonstrate that lead optimization of achiral pyrazinone-based HCV NS3 protease inhibitors is possible using elongated R^6 substituents directed toward the S2 pocket. This regards both inhibitory potency against wild-type and drug-resistant variants, as well as the pharmacokinetic (PK) properties.

CHEMISTRY

The 2(1*H*)-pyrazinone comprising HCV NS3 inhibitors were assembled in an altogether 5−7-step procedure (Scheme 1−3) via coupling of the P1P1′ amine (**8** and **10**, Scheme 1) with the P3P2 pyrazinone building blocks (Scheme 2). Final function-

dx.doi.org/10.1021/jm301887f | J. Med. Chem. 2014, 57, 1790−1801

Scheme 1. Synthesis of P1P1′ Building Blocks 8 and 10[a]

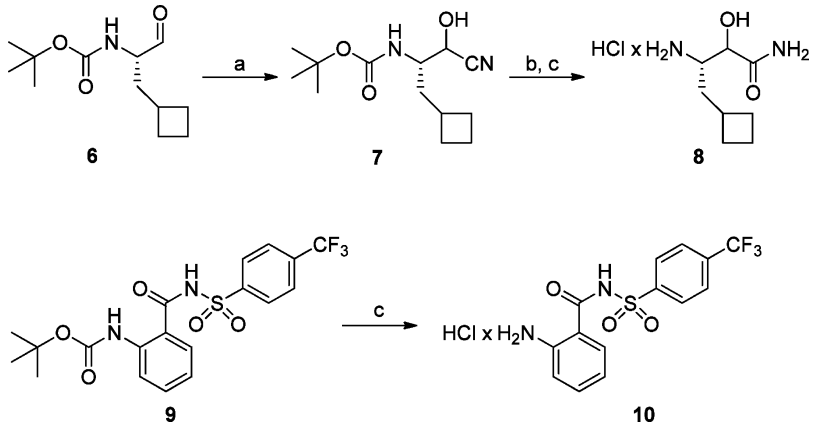

[a]Reagents and conditions: (a) KCN, acetic acid, MeOH, DCM, 0 °C, 3h (88%); (b) H_2O_2, LiOH, MeOH, 0 °C, 2 h (34%); (c) HCl in dioxane, rt, 30 min (quant).

Scheme 2. Synthesis of HCV Inhibitors 68−86[a]

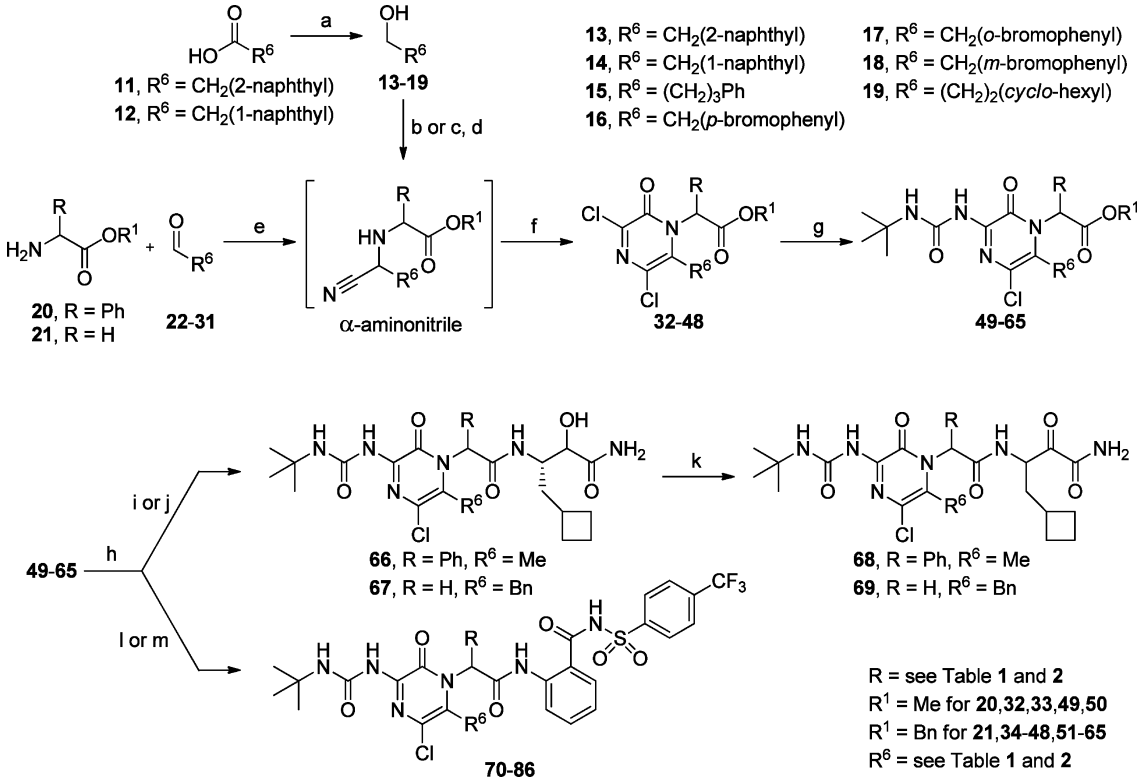

[a]Reagents and conditions: (a) $LiAlH_4$, THF, −78 °C to rt; (b) SO_3−Py, Et_3N, DMSO, DCM, rt, 1 h; (c) Dess−Martin periodinane, DCM, rt, 30 min; (d) **21**, TMSCN, DIPEA, reflux, 1 h; (e) TMSCN, DIPEA, DME, MW, 110−170 °C, 10 min or reflux, 30 min; (f) HCl gas, Et_2O, then oxalyl chloride, DME, MW, 145 °C for 25 min or reflux on (23−66% from **20** or **21**); (g) *tert*-butylurea, $Pd(OAc)_2$, Xantphos, Cs_2CO_3, DME, MW, 100−110 °C, 15−20 min or reflux, 0.5−1 h (46−89%); (h) K_2CO_3, MeCN, H_2O, MW, 110 °C, 15 min; (i) **8**, HATU, DIPEA, DMF, 0 °C, 2.5 h (**67**, 62%); (j) **8**, HATU, DIPEA, DCM, ultra sonic bath, rt, 5 min (**66**, 85%); (k) EDCI, DMSO, dichloroacetic acid, DCM, rt, 4−6 h (13−64%); (l) **10**, HATU, DIPEA, DCM, rt to 40 °C, 2.5 h (**71**, 22%); (m) **10**, $POCl_3$, pyridine, −15 °C to rt, 0.5−3 h (20−66%).

alizations of the R^6-group were done using Suzuki−Miyaura couplings (Scheme 3).

The P1 subunit **8** was synthesized starting from aldehyde **6** that was treated with potassium cyanide and acetic acid in MeOH/DCM[24] to give cyanohydrin **7**[25] (88% yield, 1:1 diastereomeric ratio, Scheme 1). Partial hydrolysis of the nitrile in a basic hydrogen peroxide solution followed by Boc deprotection gave the α-hydroxyamide unit **8** in 34% yield.[25]

The achiral acylsulfonamide building block **10** was prepared from the known carbamate **9**[21] via Boc removal in acidic dioxane.

The commercially available aldehydes **22**−**31** were used in a Strecker type reaction involving imine formation with phenylglycine methyl ester (**20**) or glycine benzyl ester (**21**) followed by cyanide addition to afford the α-aminonitriles (Scheme 2). Full consumption of **20** and **21** was reached after microwave

dx.doi.org/10.1021/jm301887f | J. Med. Chem. 2014, 57, 1790−1801

irradiation[26,27] at 110−120 °C for 10 min or reflux for 30 min, with the exception of reactions utilizing paraformaldehyde (**24**). In this case, microwave heating at 170 °C for 10 min was required to give full consumption of the amine. Alcohols **13**−**19** were used to incorporate other R^6 functionalities and 2- and 1-naphthyl ethanols **13** and **14** were obtained through reduction of the corresponding carboxylic acids **11** and **12**. Pyridine sulfur trioxide was identified as a convenient oxidizing agent that allowed a straightforward one-pot transformation of the alcohols into α-aminonitriles. Thus, the alcohols **13**−**18** were oxidized to desired aldehydes and then trapped in situ by the addition of amine **21** and trimethylsilyl cyanide to afford the desired α-aminonitriles. This protocol was used for all alcohols with the exception of the 3-cyclohexylpropanol (**19**), which was instead oxidized using the Dess−Martin periodinane reagent. The crude α-aminonitriles were then enriched with HCl gas in diethylether, followed by a solvent exchange to 1,2-dimethoxyethane (DME) and the addition of oxalyl chloride. Subsequent cyclization to the N-1, C-6-disubstituted 3,5-dichloro-2(1*H*)-pyrazinones **32**−**48** was achieved either by microwave irradiation at 145 °C for 25 min in sealed vials[28] or reflux overnight in comparable yields (25−66% over 2 or 3 steps). Unfortunately, when phenylglycine methyl ester **20** was used in the synthesis, racemization occurred during the cyclization to the 2(1*H*)-pyrazinones (**32** and **33**). Next, a chemoselective palladium-catalyzed urea *N*-arylation coupling was used to install the C-3 urea moiety.[28,29] By using $Pd(OAc)_2$ as a palladium source, Xantphos as ligand, Cs_2CO_3 as base, and *tert*-butylurea as nucleophile, the products **49**−**65** were isolated in moderate to good yields (ranging from 46 to 89%) after microwave heating at 100−110 °C for 15−20 min or reflux for 30−60 min. It is well-known that the chlorine in position C-3 can be readily substituted in numerous reactions due to the low electron density on the carbon, leaving the C-5 chlorine moiety intact.[30,31] However, it was surprising to note that complete C-3 selectivity also was achieved in the synthesis of compounds **60**−**65** (precursors to target compounds **81**−**86**, Scheme 3), comprising potentially Pd(0) reactive aryl bromide moieties, even though an excess of *tert*-butylurea (3 equiv) was used. After urea *N*-arylation, the methyl and benzyl esters were hydrolyzed, without any decomposition of the urea functionality, by microwave irradiation at 110 °C for 15 min in an aqueous solution of acetonitrile and potassium carbonate.[21] The HATU promoted peptide coupling between the carboxylic acid derived from **49**, and the building block **8** in DCM was slow and gave low yields. To better solubilize the starting materials, the use of an ultrasonic bath[32] was evaluated. This resulted in full conversion after only 5 min, and the product **66** was isolated in 85% yield. The corresponding peptide coupling to **67** was performed in DMF, which gave the α-hydroxyamide product in 62% yield. Finally, oxidation with EDCI, DMSO, and dichloroacetic acid in DCM gave the final α-ketoamides **68** and **69** in low to modest yields (13% and 64%, respectively). The low yield of **68** was mainly due to dimerization of the product during workup. To couple the acyl sulfonamide **10** with the free carboxylic acids derived from esters **49**−**65**, two peptide coupling protocols were evalutated. Because of the poor nucleophilicity of **10**, much of the starting material remained intact in the HATU promoted couplings (**71**, 22% yield). Instead, phosphoryl chloride in pyridine at low temperatures provided a more robust protocol, enabling isolation of the final inhibitors **70** and **72**−**86** in 23−66% yield.

Scheme 3 illustrates the final decoration of the aryl-bromide containing pyrazinones **81**−**86**. The final products were prepared via a microwave-assisted Suzuki−Miyaura coupling with 3-pyridylboronic acid, which gave **87**−**92** in poor to moderate yields (20−69%).[33] Even though a large excess of the boronic acid was used (5 equiv), we never observed the corresponding C-5 substitution and, furthermore, only traces of the hydrolyzed *tert*-butyl urea could be detected.

Scheme 3. Suzuki−Miyaura Cross-Couplings to Give HCV NS3 Inhibitors 87−92[a]

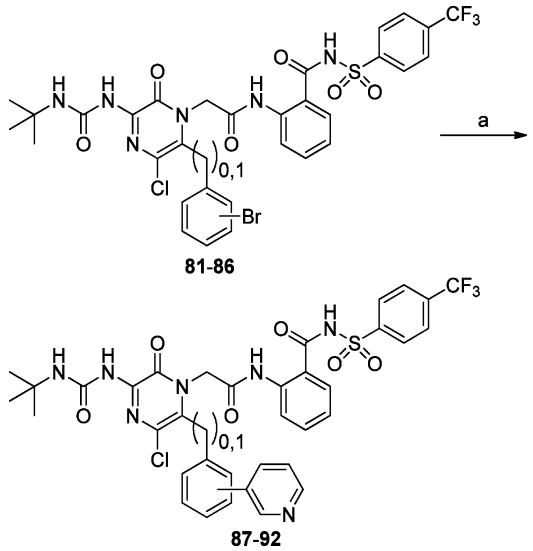

[a]Reagents and conditions: (a) 3-pyridylboronic acid, $Pd(PPh_3)_2Cl_2$, Na_2CO_3, H_2O, EtOH, DME, MW, 120 °C, 15 min (20−69%).

RESULTS

Biochemical Evaluation. The expression and purification of all enzyme variants were performed according to previously published methods.[14,34] An R155K variant ($NS3_{fl\ R155K}$[1a]), in which the arginine (R) to lysine (K) mutation was introduced by PCR at position 155, was cloned in a similar way as has been described previously.[14] The K_i values of the inhibitors **5**, **68**−**92** were obtained in an in vitro assay for the full-length NS3 protein and the central part of the NS4A as cofactor (Tables 1−2).[34] The inhibitors in this series have K_i values between 0.11−7.1 μM. Compounds **70**, **80**, and **87** were also evaluated in an in vitro assay using the full length protein with amino acid substitution A156T, D168V, or R155K, presented in Table 3. Vitality values were calculated to normalize the inhibitory effects of the inhibitors with respect to the effects from amino acid substitutions on catalytic efficiency (k_{cat}/K_m) of the enzyme variants. A vitality value less than 1 demonstrates a more efficient inhibitor against the mutated variant compared to the wild-type enzyme, while if $V > 1$, the inhibitor is less efficient against the mutated virus.[35,36] The three inhibitors evaluated possess vitality values between 0.6 and 2.0.

Calculated pK_a and log $D_{7.4}$ Values. Predictions of pK_a and log $D_{7.4}$ were performed using ADMET Predictor v.5.5. Calculated pK_a values for the acyl sulfonamide of six selected compounds in this series are found in the range of 4.7−5.1, and log $D_{7.4}$ values stretch between 3.8 and 5.0 (Table 4). From these log $D_{7.4}$ values, one could expect low solubility and moderate to high permeability for rule-of-5 compliant compounds.[37]

dx.doi.org/10.1021/jm301887f | J. Med. Chem. 2014, 57, 1790−1801

Table 1. Inhibition of the Full-Length Wild-Type NS3 Protease: Evaluation of the Carbamate to Urea Exchange and an Electrophilic versus an Acidic Product-Based P1P1′ Residue

Compound	Structure	$K_i \pm SD^a$ (μM)
5	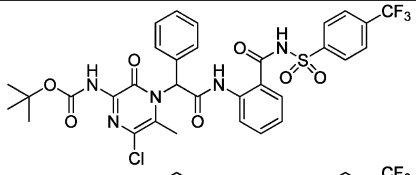	3.8 ± 0.6
70	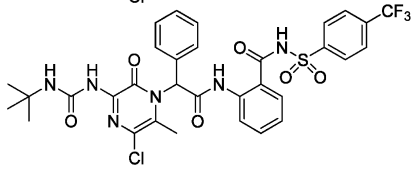	0.39 ± 0.13
68	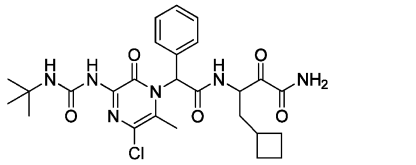	6.2 ± 0.9
71	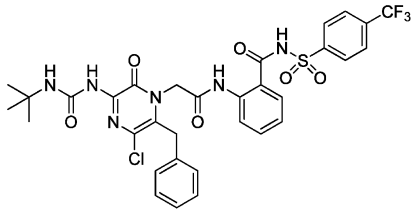	0.66 ± 0.14
69	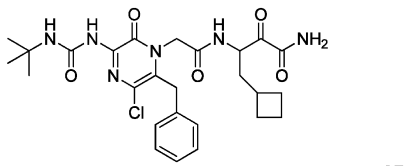	7.1 ± 1.0
72	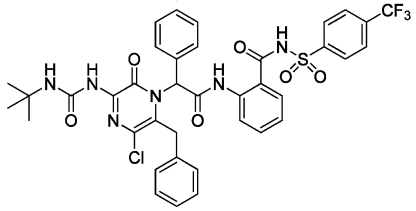	0.70 ± 0.06

[a]K_i values are the average of three separate experiments, with the standard deviation.

Table 2. Inhibition of the Full-Length Wild-Type NS3 Protease: Pyrazinone Containing HCV Inhibitors with Elongated R^6 Substituents

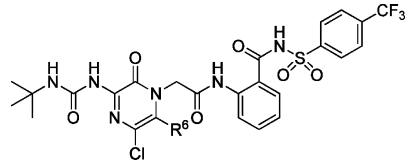

Cmpd.	R^6	$K_i \pm SD^a$ (μM)	Cmpd.	R^6	$K_i \pm SD^a$ (μM)
73		1.9 ± 1.0	**84**	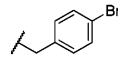	0.44 ± 0.09
71		0.66 ± 0.14	**85**		0.29 ± 0.06
74	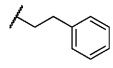	0.12 ± 0.02	**86**		0.25 ± 0.14
75	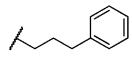	0.14 ± 0.01	**87**	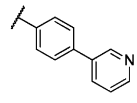	0.44 ± 0.08
76	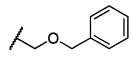	0.56 ± 0.12	**88**	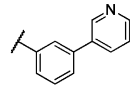	0.39 ± 0.17
77	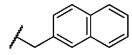	0.33 ± 0.07	**89**	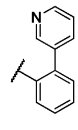	2.1 ± 0.5
78	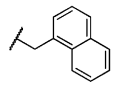	0.29 ± 0.09	**90**	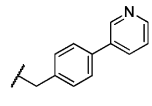	0.54 ± 0.18
79	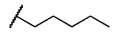	0.16 ± 0.06	**91**	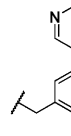	0.81 ± 0.33
80	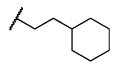	0.11 ± 0.05	**92**	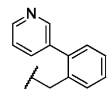	1.1 ± 0.2
81	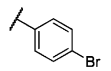	0.38 ± 0.09			
82	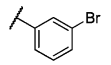	0.60 ± 0.20			
83		0.40 ± 0.25			

[a]K_i values are the average of three separate experiments, with the standard deviation.

In Vitro Physicochemical and Pharmacokinetic Profiling. Six representative compounds were selected for in vitro pharmacokinetic profiling: one from the phenylglycine series (**70**, Table 1) and five with different R^6 substituents from the glycine series (**74**, **76**, **79**, **80**, and **87**, Table 2). Solubility was determined in phosphate buffered saline (PBS) at pH 7.4 with a final concentration of DMSO of 1%. The compounds were soluble in the lower region, with solubility ranging between 21−53 μM (Table 4). The pyridine containing compound **87** was the most soluble (53 μM) in the series.

The metabolic stability was determined by incubating the compounds with pooled human liver microsomes (0.5 mg/mL, 0−40 min). In vitro half-life ($t_{1/2}$) and in vitro intrinsic clearance (Cl_{int}) were calculated using previously published models,[38,39] and the results are presented in Table 4. The Cl_{int} in microsomal incubations gives an estimation of the risk of oxidative first pass metabolism in vivo. A general classification is: Cl_{int} < 30 (μL/min/mg), no risk for high first metabolism in vivo; 30 < Cl_{int} < 92, moderate risk; Cl_{int} > 92, high risk. The inhibitors evaluated in this series showed in vitro half-life values ($t_{1/2}$) between 27 and >100 min and in vitro intrinsic clearance (Cl_{int}) between 13−52 μL/min/mg (Table 4). Thus, the pyrazinone-based HCV inhibitors tested herein show low to moderate risk of oxidative first pass metabolism.

The intestinal epithelial permeability, expressed as apparent permeability coefficients (P_{app}), was determined from transport rates across Caco-2 cell monolayers, essentially as described previously.[40] However, a modified assay based on more physiological media had to be devised because all tested compounds displayed very strong adsorption to the plastic ware. Briefly, to minimize the nonspecific binding, fasted state simulated intestinal fluid (FASSIF)[41] was used in the apical (donor) compartment and a 1% (w/v) bovine serum albumin (BSA) solution of Hank's Buffered Salt Solution (HBSS)[42] was

dx.doi.org/10.1021/jm301887f | J. Med. Chem. 2014, 57, 1790−1801

Table 3. Inhibition of the Protease Activity of Wild-Type (wt) and the A156T, D168V, and R155K Variants of the Full-Length NS3 Protease and Corresponding Vitality Values (V)

Compound	Enzyme variant	V[a]	K_i (nM)
70	A156T	2.0	930
	D168V	1.3	1260
	R155K	0.6	1550
	wt	1.0	390
80	A156T	1.3	170
	D168V	1.2	320
	R155K	0.6	420
	wt	1.0	110
87	A156T	1.4	740
	D168V	1.4	1520
	R155K	0.6	1800
	wt	1.0	440
1	A156T	480[b]	6100[b]
	D168V	0.4[b]	3.9[b]
	R155K	24	82
	wt	1.0[b]	15[b]
93	A156T	1600[b]	120[b]
	D168V	3200[b]	200[b]
	R155K	4300	24
	wt	1.0[b]	0.089[b]

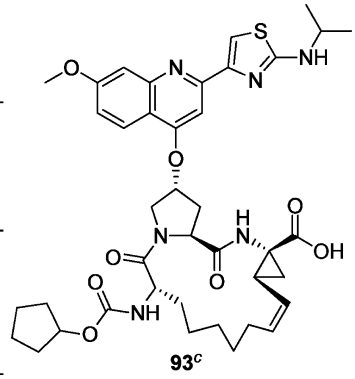

93[c]

[a]Vitality values (V) were calculated using the equation: $V = [K_i \times (k_{cat}/K_m)]_{variant}/[K_i \times (k_{cat}/K_m)]_{wild\text{-}type}$ as described by Dahl et al.[14] [b]Previously reported in Dahl et al.[14] [c]Ciluprevir/BILN2061 (**93**).

Table 4. In Vitro Pharmacokinetic Properties and in Silico pK_a Values (Acidic Acyl Sulfonamides) and log $D_{7.4}$ Values of Compounds 70, 74, 76, 79, 80, and 87

	in vitro				in silico	
			metabolic stability			
compd	solubility (μM) pH 7.4	Caco-2 Permeability P_{app} (10^{-6} cm/s)[a] a–b[b]	Cl_{int}[c] (μL/min/mg)	$t_{1/2}$[d] (min)	pK_a	log $D_{7.4}$
70	38	1.1 ± 0.4	26 ± 2	54 ± 3	4.7	4.2
74	23	0.3 ± 0.2	<13	>100	4.7	4.4
76	22	4.0 ± 1.1	17 ± 4	81 ± 19	4.7	3.8
79	21	0.04 ± 0.02	33 ± 13	42 ± 16	4.7	4.3
80	31	0.12 ± 0.09	52 ± 3	27 ± 2	4.8	5.0
87	53	7.0 ± 1.5	17 ± 3	82 ± 13	5.1	4.1

[a]P_{app} = apparent permeability coefficient. [b]a–b = apical to basolateral. [c]Cl_{int} = in vitro clearance. [d]$t_{1/2}$ = in vitro half-life.

used in the basolateral (receiver) compartment. Using this format, the experiments could be run with good mass balances above 64%. In our calibrated assay setup, a P_{app} value below 0.2 × 10^{-6} cm/s indicates low predicted intestinal permeability, a P_{app} value ranging from 0.2 × 10^{-6} cm/s to 1.6 × 10^{-6} cm/s moderate predicted intestinal permeability, and a P_{app} value above 1.6 × 10^{-6} cm/s indicates high predicted intestinal permeability.[43] The permeability data in the a–b direction showed that compounds (**70**, **74**, **76**, and **87**) displayed moderate to high permeability (ranging from 0.3 × 10^{-6} cm/s to 7.0 × 10^{-6} cm/s), while the two R^6-alkyl compounds (**79** and **80**) were poorly permeable compounds. The experimental setup prevents proper estimation of the potential efflux and P-glycoprotein interaction due to unknown interaction of the compounds with excipients and BSA, which will reduce the free concentrations of the compounds. On the other hand, the reduction in free concentrations will also result in lower estimates of the P_{app} values. Thus, the data reported in Table 4 are under rather than over predictions of the true intestinal permeability.

Molecular Modeling. The recently released HCV NS3/4A protease-helicase crystal structure in complex with a macrocyclic protease inhibitor (PDB code 4A92) was used for the molecular modeling studies.[44] The active site is situated in the boundary between the protease and the helicase domain. This is the first published cocrystal structure of the full-length NS3 protein structure and an inhibitor. The inhibitor displays not only intermolecular interactions with the protease domain but also to the helicase domain. This data is in agreement with our previous docking protocols and studies, which have often indicated some influence from the helicase domain on protease inhibitor binding.[45] Thus, this X-ray structure was particularly useful for studying possible interactions between the R^6 substituents and the S2 pocket of the protein, which is partly

dx.doi.org/10.1021/jm301887f | J. Med. Chem. 2014, 57, 1790–1801

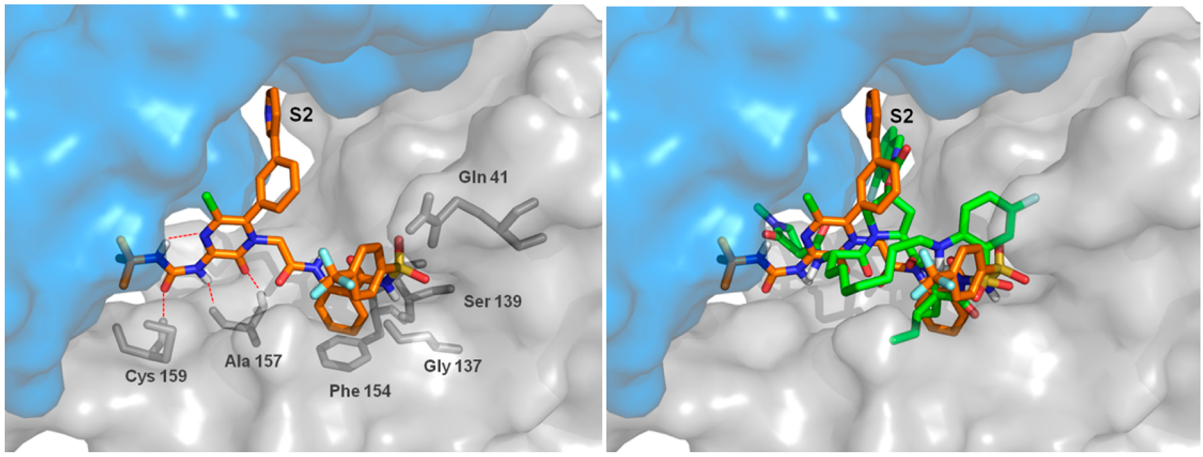

Figure 3. (A) Compound **88** modeled into the NS3 protease active site (gray surface) of the 4A92 crystal structure. The NS3 helicase domain is shown in blue surface. Key hydrogen bond interactions are highlighted as red dashed lines. The inhibitor shows π-interactions with Phe154 and Gln41. (B) Compound **88** (orange carbons) overlaid with the cocrystallized macrocyclic inhibitor (green carbons).

comprised of the helicase domain.[44] The inhibitors were modeled into the protease active site according to the protocol described in the Supporting Information. In the validation process of the modeled inhibitors, β-strand mimetics with the protein backbone were considered. This mimetic is maintained by a hydrogen-bond pattern between the CO and NH of the pyrazinone ring and the backbone of Ala157. Molecular modeling showed that the substituents in the R^6 position fit nicely into the S2 pocket. Compound **88** in Figure 3A shows a representative binding mode of the modeled inhibitors into the protein active site. The binding mode shows maintenance of the hydrogen-bond pattern between the CO and NH of the pyrazinone ring of compound **88** and the backbone of Ala157, edge-to-face interaction between the aromatic P1 moiety and Phe154, a possible π-stacking interaction between the P1′ moiety and Gln41, and an internal hydrogen bond from the urea NH to the pyrazinone. Furthermore, compound **88** was overlaid with the macrocyclic inhibitor in the X-ray structure (Figure 3B), where it can be seen that the R^6 substituent of inhibitor **88** reaches up to the S2 pocket in consistency with the P2 moiety of the cocrystallized inhibitor.

DISCUSSION

With the overall aim of developing HCV NS3 protease inhibitors different from the advanced and widely explored peptide-based compounds with a central P2 proline or a proline mimic (see, e.g., compounds **1**−**4**, Figure 1), we wanted to explore a pyrazinone ring combined with an amino acid as a central P3P2 scaffold in HCV NS3 protease inhibitors. The preliminary inhibitors (e.g., compound **5**, Figure 2) were evaluated as product-based inhibitors, meaning encompassing an acidic P1P1′ group, an acyl sulfonamide, but yet without a large P2 extension. Potent product-based inhibitors normally require a big P2 substituent to occupy the large S2 pocket (see compounds **3** and **4**). This is in contrast to the electrophilic (serine trapping) compounds, such as **1** and **2**, having smaller P2 groups. Therefore, we felt prompted to further explore pyrazinone-based compounds in two ways: either encompassing an electrophilic P1P1′ group or an acidic P1P1′ group combined with an expanded P2 substituent. Furthermore, a carbamate functionality had previously been identified as the most promising capping group (R^3 group) of the pyrazinone in terms of inhibition potency but it was accompanied with instability problems.[21]

Consequently, the first modification made on this series of compounds was to replace the carbamate group with a more stable urea functionality (Table 1). The exchange resulted in compound **70**, containing a *tert*-butyl urea, which not only proved to be more robust but also showed an impressive 10-fold improvement in potency (K_i = 0.39 μM) compared to compound **5** (K_i = 3.8 μM). Part of the potency enhancement could be related to entropy gain from potential hydrogen bonding between the urea and the pyrazinone nitrogen, as suggested from molecular modeling (see Figure 3A). Hence, the *tert*-butyl urea was successfully used throughout the series synthesized in this study. Regarding the P1P1′ unit, we decided to further explore the aromatic acyl sulfonamide (**5**, **70**−**72**, Table 1), and the same electrophilic α-ketoamide as in compound **2** (**68** and **69**, Table 1). In combination with the pyrazinone structure, the α-ketoamide functionality was less favorable (10-fold) as compared to the aromatic acyl sulfonamide residue (**68** and **69**, K_i = 6.2 and 7.1 μM vs **70** and **71**, K_i = 0.39 and 0.66 μM, respectively). These compounds were also used to confirm the possibility to reach the S2 pocket from the R^6 position of the pyrazinone core (i.e., moving the P2 side chain to the R^6 position of the P3 pyrazinone), as suggested by modeling (Figure 3). Gratifyingly, almost equipotent glycine compounds **69** and **71** (K_i = 7.1 μM and 0.66 μM, respectively) were achieved compared to the corresponding phenylglycine compounds **68** and **70** (K_i = 6.2 and 0.39 μM, respectively). These results posed an obvious question; whether it is possible to benefit from both the phenyl glycine and a benzyl in the R^6 position or if they should occupy the same pocket. Compound **72** (K_i = 0.70 μM) was synthesized accordingly but showed no advantages over the glycine-based inhibitors. Therefore, we were encouraged to further explore achiral inhibitors and improve inhibitory potency via optimizations of the R^6 substituents of the pyrazinone.

The structure−activity relationship of the R^6 group was studied with preserved functionalities in the rest of the structure, i.e., the *tert*-butyl urea on the R^3 position in

dx.doi.org/10.1021/jm301887f | J. Med. Chem. 2014, 57, 1790−1801

combination with the aromatic P1P1′ scaffold (see compounds **73**−**92**, Table 2). The R^6 substituents were chosen to address the preferred length and direction of the substituent in this new type of inhibitors. Hence, elongated phenyl containing substituent of different linker lengths and corresponding alkyl substituents were evaluated, as were naphthyl and various bromo- and pyridine-substituted phenyl and benzyl substituents. Overall, it is clear that the R^6 substituent occupies a rather large lipophilic pocket because the inhibitory potency is enhanced by several of the larger substituents with K_i values down to 0.11 μM (**80**). However, interactions are not completely unspecific because elongations in some directions are not allowed, exemplified by the *ortho*-pyridyl comprising **89** and **92** (K_i = 2.1 and 1.1 μM, respectively). In line with this, the inhibitory potency decreased considerably in the absence of an R^6 group, as demonstrated by compound **73** (K_i = 1.9 μM) compared to benzyl **71** (K_i = 0.66 μM). Elongation of the benzyl compound **71** via a methylene spacer gave phenethyl **74** with a 5-fold improved potency (K_i = 0.12 μM), and further elongation by one carbon resulted in comparable inhibitory potency (**75**, K_i = 0.14 μM). Replacing a methylene with an oxygen gave the less hydrophobic compound **76** (K_i = 0.56 μM), but this alteration resulted in a less potent inhibitor. The corresponding naphthyl groups gave somewhat less potent inhibitors (**77**, K_i = 0.33 μM and **78**, K_i = 0.29 μM), however, compared to benzyl **71**, this alteration was well accepted.

Molecular modeling suggested that a R^6 phenyl equipped with bulky substituents (e.g., a pyridyl, Figure 3) could establish important interactions with the S2 pocket. Consequently, we decided to synthesize bromoaryls as intermediate inhibitors that also should allow further functionalization using metal catalyzed cross coupling reactions. The *ortho*-, *meta*-, and *para*-bromo phenyl analogues **81**−**83** (K_i = 0.38, 0.60, and 0.40 μM, respectively) provided improved or similar inhibitory potencies as the benzyl compound **71** (K_i = 0.66 μM), although, from these results, the preferred direction of the substituent on the aryl could not be identified. The R^6 bromo-benzyl analogues **84**−**86** (K_i = 0.44, 0.29, and 0.25 μM, respectively) showed a slight overall enhanced or similar inhibitory potencies compared to the corresponding analogous phenyl. Again, there was no clear preference for a particular regioisomer. We anticipated that introduction of a heteroaromatic group in these positions could be useful in order to reach interactions with the S2 pocket as well as influence the pharmacokinetic properties and solubility. The majority of the HCV NS3 protease inhibitors in clinical studies contain a heteroaromatic P2 substituent which has proven beneficial for activity and pharmacokinetic properties.[8,46] Thus, compounds **87**−**92** were prepared comprising *ortho*-, *meta*-, and *para*-3-pyridyls, however, no significant improvement in potency was observed. Interestingly, an *ortho*-pyridyl was not well tolerated, giving a 4−5-fold decrease in potency compared with the *ortho*-bromo equivalents (e.g., **83**, K_i = 0.40 μM vs **89**, 2.1 μM, and **86**, 0.25 μM vs **92**, 1.1 μM). According to molecular modeling (see Figure S1, Supporting Information), the *ortho*-bromo compounds seem to direct the bromo-substituent into the S2 pocket in analogy with the majority of the compounds in the series (i.e., *meta* and *para*). However, for the inhibitors with the pyridyl substituent in the *ortho* position, modeling suggests poses where the pyridyl group is directed in the opposite direction, i.e., out from the S2 pocket, and instead forming hydrophobic interaction with the inhibitor itself. In these poses, a distortion of the inhibitor backbone is also seen, which altogether may account for the loss in inhibitory potency.

The high aromatic ring content raised concerns about potential pharmacokinetic issues as it is considered to be less suitable in a bioavailable drug candidate.[47−49] Hence, we speculated if a simple alkyl chain could retain the potency possessed by their aromatic counterparts. Indeed, the pentyl containing compound **79** revealed an impressive inhibitory potency (K_i = 0.16 μM) comparable with the most potent aromatic analogue (phenethyl **74**, K_i = 0.12 μM). In analogy, the corresponding cyclohexyl variant **80** (K_i = 0.11 μM) turned out to be the most potent inhibitor in this set of compounds. The total SAR accomplished from the R^6 substituent study in Table 2 indicates that the potency loss suffered from removal of the classical P2 side chain indeed could be regained by elongation of a variety of lipophilic, but not too sterically hindered, R^6 substituents. Consequently, there is a freedom for the actual lead optimization strategy chosen for the R^6 group to be guided by other drug properties, i.e., resistance profile or pharmacokinetic data.

Substitutions of the residues at positions 155, 156, and 168 in the HCV NS3 protease are among the most frequently observed mutations in vitro and in vivo during clinical studies evaluating HCV NS3 protease inhibitors.[50] These resistance mutations impair the efficacy of the direct-acting antiviral drugs on the market as well as those in clinical trials.[12,50,51] Because there is a risk for cross-resistance,[12] future NS3 protease inhibitors should be designed to retain potency against cross-resistant enzyme variants. Accordingly, three inhibitors **70**, **80**, and **87**, were selected for evaluation toward the resistant enzyme variants A156T, D168V, and R155K (Table 3). The compounds were chosen based on their promising inhibitory potencies and their structural diversity: one compound from the phenylglycine series (**70**) and one alkyl and aromatic analogue from the achiral glycine series (**80** and **87**). It is reported that mutations leading to amino acid substitutions at Ala156 cause resistance to most of the evaluated HCV NS3 protease inhibitors.[12,52,53] These mutations result in increased bulk and steric repulsion between the enzyme and the P2 and P4 residues of the inhibitor.[53] It is inaccurate to compare inhibition constants (K_i values) between enzyme variants of different catalytic efficiencies (k_{cat}/K_m). Therefore, vitality values (V) that normalize for this were calculated (Table 3). The first proof-of-concept HCV NS3 protease inhibitor **93** (Ciluprevir/BILN2061)[54] loses inhibitory potency dramatically against the A156T variant, showing a vitality value of 1600. Also, inhibitor **1** loses inhibitory potency substantially, with a vitality value of 480. According to the vitality values for inhibition of the A156T variant, the inhibitors **70**, **80**, and **87** were able to retain most of their inhibition potency in relation to the wild-type enzyme. Interestingly, the achiral inhibitors **80** (V = 1.3) and **87** (V = 1.4) showed a more promising potency compared to the racemic inhibitor **70** with a V value of 2.0. The D168V mutated form of the protease is known to dramatically affect macrocyclic inhibitors with large P2 substituents.[52,55] This is supported by a vitality value of 3200 for macrocyclic inhibitor **93**, comprising a bulky P2 group, and a vitality value of 0.4 for the linear inhibitor **1** lacking a large P2 group. Asp168 is positioned between the S2 and the S4 pocket and forms salt bridges to Arg123 in S4 and Arg155 in S2. A mutation at Asp168 disrupts the stabilizing effect and leads to weaker interactions of the inhibitor with the S2 and S4 pockets.[11,53] Evaluation against the D168V mutated form resulted in vitality

values close to 1, which implies maintained efficacy compared to the wild-type enzyme. This may be due to the smaller size of the P2 substituent, which will suffer less from changes in the S2 pocket. Arg155 is positioned in the S2 pocket and thereby has the ability to interact with large P2 substituents. Mutations leading to substitutions at the Arg155 position appear to be most crucial presently because they lead to cross-resistance to all HCV NS3 protease inhibitors in advanced clinical development.[12] The potencies for both reference substances, **1** and **93**, were indeed negatively affected by amino acid substitution R155K (V = 24 and 4300, respectively). Amino acid substitutions at this position could disrupt the previously mentioned salt bridge with Asp168, resulting in resistance to inhibitors with interactions in this region.[11,53] Evaluation of the three inhibitors **70**, **80**, and **87** against R155K produced encouraging results. The vitality values were determined to be less than 1, indicating that these early stage inhibitors are more efficient against the mutated form compared to the wild-type enzyme. Thus, the pyrazinone-based inhibitors can be regarded as promising lead compounds in terms of drug resistance profile. However, further improvements in the overall inhibitory potencies are still highly warranted.

The in vitro solubility, metabolic stability, and permeability were determined for six representative compounds: one from the phenylglycine series (**70**) and five from the achiral glycine series (**74**, **76**, **79**, **80**, and **87**), as shown in Table 4. We hoped that such data could aid future development of the lead compounds derived herein. All evaluated inhibitors have solubility higher than 20 μM (corresponds roughly to >15 μg/mL), which imply that solubility is not a major problem for this series of inhibitors. Nevertheless, the extensive adsorption seen with plastics in the Caco-2 assay implies that care must be taken when designing in vitro experiments for this type of lipophilic peptidomimetics. Considering that the pyridine comprising analogue **87** was the most soluble (56 μM/44 μg/mL), modifications using pyridines or other heteroaryls should be considered in future designed inhibitors. The in vitro intrinsic clearance measurement, performed in human liver microsomes of the compounds, indicated a low or moderate risk for high oxidative first pass metabolism in vivo for this class of compounds. This is pleasing results given their high lipophilicity (log $D_{7.4}$ = 3.8−5.0), high molecular weight (700−785 g/mol), and aromatic nature. In addition, the pyrazinone-based compounds with alkyls in R^6 position (**79** and **80**) are metabolically less stable than the corresponding aryl comprising analogues (**74**, **76**, and **87**), with intrinsic clearance values of >30 μL/min/mg (apparent moderate risk) in the former cases and <20 μL/min/mg (apparent no risk) in the latter cases. Finally, the permeability data shown in Table 4 indicate widely different permeabilities of the compounds, although they only differ in the R^6 position. The two alkyl comprising compounds **79** and **80** displayed low permeability, and the phenylglycine compound **70** and the glycine analogue with a phenethyl R^6 substituent **74** displayed moderate permeability, whereas the two compounds comprising one heteroatom in the R^6 group, i.e., the ether analogue **76** and the pyridyl analogue **87** were highly permeable compounds. Thus, the presence of a pyridine has a positive influence on the in vitro pharmacokinetic properties in general. Notably, the modified Caco-2 assay mimics both the intestinal compartment in the donor chamber and the blood in the receiving compartment. The tradeoff is that at present accurate determination of the free compound concentrations, driving permeability and active efflux of these compounds, cannot be estimated.

CONCLUSION

The evaluated series of peptidomimetic HCV NS3 protease inhibitors based on a P3 2(1*H*)-pyrazinone scaffold benefited from an aryl acyl sulfonamide-based P1P1′ group, in contrast to corresponding electrophilic α-keto amides. A key improvement was further achieved by an exchange of an unstable carbamate P3 capping group to a robust urea, which resulted in a 10-fold increase in inhibitory potency. Results from the SAR study indicated that the P2 side chain could be transferred to the R^6 position on the P3 pyrazinone, giving achiral structures, and further optimized using lipophilic but not too sterically hindered substituents. Furthermore, the same substituents were found to significantly influence the pharmacokinetic properties of the compounds. Even though aliphatic R^6 substituents were allowed in terms of potency, contrasting results were achieved from pharmacokinetic evaluations, which instead revealed a beneficial effect of a 3-pyridyl group. Accordingly, further elaboration in this position is warranted and is currently underway in our laboratory. Indeed, the developed synthetic pathway enables a wide variety of structural modifications to be performed in the future design of improved inhibitors. Evaluation of the inhibitors against drug-resistant variants of the full-length NS3 protease revealed retained inhibitory potencies compared to the wild-type enzyme. Taken together, these results combined with the unique structural features and promising in vitro pharmacokinetic properties prompt further optimization of this novel class of achiral drug leads.

EXPERIMENTAL SECTION

General Methods. Microwave-assisted reactions were performed in sealed vials dedicated for microwave processing, using a Smith synthesizer. NMR spectra were recorded on a Varian Mercury Plus for ^{1}H at 399.9 MHz and for ^{13}C NMR at 100.5 MHz. Analytical HPLC-UV/MS analysis of pure products were performed on a Gilson HPLC system with a Chromolith SpeedROD RP-18e column (50 mm × 4.6 mm) equipped with a Finnigan AQA quadrupole mass spectrometer using a 4 mL/min MeCN/H_2O gradient (0.05% HCOOH) and detection by UV (DAD) and MS (ESI+). All compounds were determined to be >95% pure by HPLC-UV at 254 nm.

Representative Total Synthesis of an Inhibitor (Compound 80). *Benzyl 2-(3,5-Dichloro-6-(2-cyclohexylethyl)-2-oxopyrazin-1(2H)-yl)acetate (40).* A 50 mL round-bottom flask was loaded with 3-cyclohexyl-1-propanol (0.55 g, 3.87 mmol), dry DCM (25 mL), and Dess−Martin periodinane (1.64 g, 3.87 mmol). The reaction was stirred in rt for 30 min and then washed with 25 mL of saturated $NaHCO_3$, dried over $MgSO_4$, and evaporated. A solution of glycine benzyl ester hydrochloride (0.65 g, 3.22 mmol) and DIPEA (0.70 mL, 4.02 mmol) in DCM (25 mL) was added to the crude residue. Trimethylsilyl cyanide (0.45 mL, 3.54 mmol) was added after 0.5 min, and the reaction was refluxed for 1 h. The solvent was removed under reduced pressure and the residue flushed through a silica plug and eluted with EtOAc:isohexane (20:80). The crude residue was taken up in 15 mL of diethyl ether and transferred to a 20 mL Smith vial. HCl gas was bubbled through the reaction mixture for 5 min, followed by evaporation of the solvent. Oxalyl chloride (0.85 mL, 9.68 mmol) and DME (10 mL) was added, and the vial was capped and irradiated with MW to 145 °C for 25 min.[28] The crude product was, after evaporation of the solvent, purified by silica column flash chromatography using EtOAc:isohexane (10:90 to 30:70) as eluent and gave **40** in 28% yield, 0.38 g as pale-yellow solid. ^{1}H NMR ($CDCl_3$) δ 7.38−7.30 (m, 5H), 5.21 (s, 2H), 4.80 (s, 2H), 2.58 (m, 2H), 1.73−1.61 (m, 5H), 1.36 (m, 2H), 1.31 (m, 4H), 0.93−0.80 (m, 2H). ^{13}C NMR ($CDCl_3$) δ 166.0,

152.6, 143.2, 139.5, 134.6, 128.8, 128.7, 128.5, 123.5, 68.1, 47.3, 37.5, 34.2, 32.7, 27.8, 26.3, 26.0. ESI-MS (m/z) 423 ($M + H^+$). HRMS calcd for $C_{21}H_{24}Cl_2N_2O_3$ ($M + H^+$) 423.1242; found 423.1237.

*Benzyl 2-(3-(3-(tert-Butyl)ureido)-5-chloro-6-(2-cyclohexylethyl)-2-oxopyrazin-1(2H)-yl)acetate (**57**).* A 5 mL microwave process vial was charged with **40** (210 mg, 0.50 mmol), *tert*-butylurea (290 mg, 2.50 mmol), $Pd(OAc)_2$ (6 mg, 0.03 mmol), Xantphos (23 mg, 0.04 mmol), Cs_2CO_3 (325 mg, 1.00 mmol), and DME (5 mL). The vial was capped under air, and the reaction mixture was irradiated with MW to 100 °C for 15 min. The solids were filtered off and the residue concentrated under reduced pressure. The crude product was purified by silica column flash chromatography and eluted with EtOAc:isohexane (15:85 to 30:70) to afford **57** in 72% yield, 181 mg as white solid. ^{1}H NMR ($CDCl_3$) δ 8.55 (br s, NH), 7.88 (br s, NH), 7.39−7.30 (m, 5H), 5.20 (s, 2H), 4.77 (s, 2H), 2.51 (m, 2H), 1.72−1.61 (m, 5H), 1.41 (s, 9H), 1.32 (m, 2H), 1.27−1.08 (m, 4H), 0.92−0.81 (m, 2H). ^{13}C NMR ($CDCl_3$) δ 166.4, 151.4, 150.7, 143.7, 134.7, 128.9, 128.8, 128.7, 128.5, 122.4, 68.0, 51.0, 46.3, 37.5, 35.0, 32.8, 28.9, 27.1, 26.4, 26.1. ESI-MS (m/z) 503 ($M + H^+$). HRMS calcd for $C_{26}H_{35}ClN_4O_5$ ($M + H^+$) 503.2425; found 503.2420.

*2-(2-(3-(3-(tert-Butyl)ureido)-5-chloro-6-(2-cyclohexylethyl)-2-oxopyrazin-1(2H)-yl)acetamido)-N-((4-(trifluoromethyl)phenyl)sulfonyl)benzamide (**80**).* A 5 mL microwave process vial was charged with **57** (125 mg, 0.25 mmol), K_2CO_3 (70 mg, 0.51 mmol), MeCN (2.0 mL), and H_2O (1.0 mL), and the vial was capped and irradiated by MW to 110 °C for 15 min. After cooling to rt, 1.0 M HCl (20 mL) was added and the mixture was extracted with EtOAc (2 × 20 mL). The organic layers were dried over $MgSO_4$ and evaporated.[21] The crude acid and **6** (143 mg, 0.38 mmol) were dissolved in pyridine (4 mL) and cooled to −15 °C under N_2 atmosphere. $POCl_3$ (26 μL, 0.28 mmol) was added, and the reaction mixture was stirred at −15 °C for 15 min before removal of the cold bath. After 30 min stirring in rt, water (20 mL) was added and the pH adjusted to 1 using 6.0 M HCl followed by extraction with EtOAc (2 × 20 mL). The organic layer was dried over $MgSO_4$ and evaporated, and the crude product was purified by silica column flash chromatography two times, first eluting with EtOAc:isohexane:HCOOH (20:80:3 to 30:70:3), and in the second column the product was eluted with MeOH:DCM (1:100 to 3:100), which gave **80** in 14% yield, 26 mg as white solid. ^{1}H NMR ($(CD_3)OD$) δ 8.32 (m, 1H), 8.20 (m, 2H), 8.04 (m, 1H), 7.69 (m, 2H), 7.32 (m, 1H), 6.93 (m, 1H), 4.97 (m, 2H), 2.68 (m, 2H), 1.67−1.49 (m, 5H), 1.40 (s, 9H), 1.37−1.30 (m, 2H), 1.23−0.99 (m, 4H), 0.87−0.73 (m, 2H). ^{13}C NMR (CD_3OD) δ 175.1, 166.0, 153.8, 152.3, 148.7, 144.9, 140.8, 133.9 (q, J = 32 Hz), 133.3, 132.6, 132.2, 129.5, 128.7, 126.6, (q, J = 3.8 Hz), 125.1 (q, J = 272 Hz), 124.1, 123.4, 121.0, 52.0, 50.8, 38.6, 35.9, 34.0, 29.2, 28.3, 27.5, 27.2. ESI-MS (m/z) 739 ($M + H^+$). HRMS calcd for $C_{33}H_{38}ClF_3N_6O_6S$ ($M + H^+$) 739.2292; found 739.2300.

■ ASSOCIATED CONTENT

Supporting Information

Additional experimental details concerning synthesis, characterization, and spectra (^{1}H, ^{13}C NMR, LC-UV/MS) of novel compounds (**33**, **34**, **36**−**92**), inhibition assay, molecular modeling, metabolic stability assay, and solubility determination. This material is available free of charge via the Internet at http://pubs.acs.org.

■ AUTHOR INFORMATION

Corresponding Author

*Phone: 46-18-471-4957. Fax: 46-18-471-4474. E-mail: Anja.Sandstrom@orgfarm.uu.se.

Author Contributions

#J.G. and A.K.B. contributed equally. The manuscript was written through contributions of all authors. All authors have given approval to the final version of the manuscript.

Notes

The authors declare no competing financial interest.

■ ACKNOWLEDGMENTS

We thank Johan Gustafson for the synthesis of compounds **36**, **39** and **40**, and Benjamin Schmuck and Alexander Sachse for their assistance in the construction, expression, and purification of the R155K HCV NS3 variant and Dr. Luke R. Odell for constructive proofreading of the manuscript. We also thank Simulations Plus for providing access to the ADMET Predictor software and the Swedish Research Council and Alice Wallenberg Foundation for financial support.

■ ABBREVIATIONS USED

HCV, hepatitis C virus; DME, dimethoxyethane; Xantphos, 4,5-bis(diphenylphosphino)-9,9-dimethylxanthene; HATU, 1-[bis(dimethylamino)methylene]-1*H*-1,2,3-triazolo[4,5-*b*]-pyridinium 3-oxid hexafluorophosphate; EDCI, 3-(ethyliminomethyleneamino)-*N*,*N*-dimethylpropan-1-amine. Cl_{int}, intrinsic clearance; P_{app}, apparent permeability coefficient

■ REFERENCES

(1) Gravitz, L. A smouldering public-health crisis. *Nature* **2011**, *474*, S2−S4.

(2) *Hepatitis C: Fact Sheet no. 164*; World Health Organization: Geneva, June, 2011.

(3) Eisenstein, M. A moving target. *Nature* **2011**, *474*, S16−S17.

(4) Soriano, V.; Vispo, E.; Poveda, E.; Labarga, P.; Martin-Carbonero, L.; Fernandez-Montero, J. V.; Barreiro, P. Directly acting antivirals against hepatitis C virus. *J. Antimicrob. Chemoth.* **2011**, *66*, 1673−1686.

(5) Fried, M. W.; Hadziyannis, S. J. Treatment of chronic hepatitis C infection with peginterferons plus ribavirin. *Semin. Liver Dis.* **2004**, *24*, 47−54.

(6) Lin, K.; Perni, R. B.; Kwong, A. D.; Lin, C. VX-950, a novel hepatitis C virus (HCV) NS34A protease inhibitor, exhibits potent antiviral activities in HCV replicon cells. *Antimicrob. Agents Chemother.* **2006**, *50*, 1813−1822.

(7) Malcolm, B. A.; Liu, R.; Lahser, F.; Agrawal, S.; Belanger, B.; Butkiewicz, N.; Chase, R.; Gheyas, F.; Hart, A.; Hesk, D.; Ingravallo, P.; Jiang, C.; Kong, R.; Lu, J.; Pichardo, J.; Prongay, A.; Skelton, A.; Tong, X.; Venkatraman, S.; Xia, E.; Girijavallabhan, V.; Njoroge, F. G. SCH 503034, a mechanism-based inhibitor of hepatitis C virus NS3 protease, suppresses polyprotein maturation and enhances the antiviral activity of alpha interferon in replicon cells. *Antimicrob. Agents Chemother.* **2006**, *50*, 1013−1020.

(8) Raboisson, P.; de Kock, H.; Rosenquist, Å.; Nilsson, M.; Salvador-Oden, L.; Lin, T. I.; Roue, N.; Ivanov, V.; Wähling, H.; Wickström, K.; Hamelink, E.; Edlund, M.; Vrang, L.; Vendeville, S.; Van de Vreken, W.; McGowan, D.; Tahri, A.; Hu, L. L.; Boutton, C.; Lenz, O.; Delouvroy, F.; Pille, G.; Surleraux, D.; Wigerinck, P.; Samuelsson, B.; Simmen, K. Structure−activity relationship study on a novel series of cyclopentane-containing macrocyclic inhibitors of the hepatitis C virus NS3/4A protease leading to the discovery of TMC435350. *Bioorg. Med. Chem. Lett.* **2008**, *18*, 4853−4858.

(9) White, P. W.; Llinas-Brunet, M.; Amad, M.; Bethell, R. C.; Bolger, G.; Cordingley, M. G.; Duan, J. M.; Garneau, M.; Lagace, L.; Thibeault, D.; Kukolj, G. Preclinical Characterization of BI 201335, A C-Terminal Carboxylic Acid Inhibitor of the Hepatitis C Virus NS3-NS4A Protease. *Antimicrob. Agents Chemother.* **2010**, *54*, 4611−4618.

(10) Schlutter, J. New drugs hit the target. *Nature* **2011**, *474*, S5−S7.

(11) Trozzi, C.; Bartholomew, L.; Ceccacci, A.; Biasiol, G.; Pacini, L.; Altamura, S.; Narjes, F.; Muraglia, E.; Paonessa, G.; Koch, U.; De Francesco, R.; Steinkuhler, C.; Migliaccio, G. In vitro selection and characterization of hepatitis C virus serine protease variants resistant to an active-site peptide inhibitor. *J. Virol.* **2003**, *77*, 3669−3679.

(12) Sarrazin, C.; Zeuzem, S. Resistance to Direct Antiviral Agents in Patients With Hepatitis C Virus Infection. *Gastroenterology* **2010**, *138*, 447−462.
(13) Thompson, A. J.; Locarnini, S. A.; Beard, M. R. Resistance to anti-HCV protease inhibitors. *Curr. Opin. Virol.* **2011**, *1*, 599−606.
(14) Dahl, G.; Sandström, A.; Åkerblom, E.; Danielson, U. H. Resistance profiling of hepatitis C virus protease inhibitors using full-length NS3. *Antiviral Ther.* **2007**, *12*, 733−740.
(15) Örtqvist, P.; Verna, A.; Ehrenberg, A. E.; Dahl, G.; Rönn, R.; Åkerblom, E.; Karlén, A.; Danielson, U. H.; Sandström, A. Structure−activity relationships of HCV NS3 protease inhibitors evaluated on the drug-resistant variants A156T and D168V. *Antiviral Ther.* **2010**, *15*, 841−852.
(16) Sarrazin, C.; Vermehren, J. New Hepatitis C Therapies in Clinical Development. *Eur. J. Med. Res.* **2011**, *16*, 303−314.
(17) Kwong, A. D.; Sarrazin, C.; Kieffer, T. L.; Bartels, D.; Hanzelka, B.; Muh, U.; Welker, M.; Wincheringer, D.; Zhou, Y.; Chu, H. M.; Lin, C.; Weegink, C.; Reesink, H.; Zeuzem, S. Dynamic hepatitis C virus genotypic and phenotypic changes in patients treated with the protease inhibitor telaprevir. *Gastroenterology* **2007**, *132*, 1767−1777.
(18) Örtqvist, P.; Peterson, S. D.; Åkerblom, E.; Gossas, T.; Sabnis, Y. A.; Fransson, R.; Lindeberg, G.; Danielson, U. H.; Karlén, A.; Sandström, A. Phenylglycine as a novel P2 scaffold in hepatitis C virus NS3 protease inhibitors. *Bioorg. Med. Chem.* **2007**, *15*, 1448−1474.
(19) Lampa, A.; Ehrenberg, A. E.; Gustafsson, S. S.; Vema, A.; Åkerblom, E.; Lindeberg, G.; Karlén, A.; Danielson, U. H.; Sandström, A. Improved P2 phenylglycine-based hepatitis C virus NS3 protease inhibitors with alkenylic prime-side substituents. *Bioorg. Med. Chem.* **2010**, *18*, 5413−5424.
(20) Lampa, A.; Ehrenberg, A. E.; Vema, A.; Åkerblom, E.; Lindeberg, G.; Danielson, U. H.; Karlén, A.; Sandström, A. P2−P1′ macrocyclization of P2 phenylglycine based HCV NS3 protease inhibitors using ring-closing metathesis. *Bioorg. Med. Chem.* **2011**, *19*, 4917−4927.
(21) Örtqvist, P.; Gising, J.; Ehrenberg, A. E.; Vema, A.; Borg, A.; Karlén, A.; Larhed, M.; Danielson, U. H.; Sandström, A. Discovery of achiral inhibitors of the hepatitis C virus NS3 protease based on 2(1*H*)-pyrazinones. *Bioorg. Med. Chem.* **2010**, *18*, 6512−6525.
(22) Zhang, X. J.; Schmitt, A. C.; Jiang, W.; Wasserman, Z.; Decicco, C. P. Design and synthesis of potent, non-peptide inhibitors of HCVNS3 protease. *Bioorg. Med. Chem. Lett.* **2003**, *13*, 1157−1160.
(23) Parlow, J. J.; Case, B. L.; Dice, T. A.; Fenton, R. L.; Hayes, M. J.; Jones, D. E.; Neumann, W. L.; Wood, R. S.; Lachance, R. M.; Girard, T. J.; Nicholson, N. S.; Clare, M.; Stegeman, R. A.; Stevens, A. M.; Stallings, W. C.; Kurumbail, R. G.; South, M. S. Design, parallel synthesis, and crystal structures of pyrazinone antithrombotics as selective inhibitors of the tissue factor VIIa complex. *J. Med. Chem.* **2003**, *46*, 4050−4062.
(24) Myers, A. G.; Zhong, B. Y.; Kung, D. W.; Movassaghi, M.; Lanman, B. A.; Kwon, S. Synthesis of C-protected alpha-amino aldehydes of high enantiomeric excess from highly epimerizable N-protected alpha-amino aldehydes. *Org. Lett.* **2000**, *2*, 3337−3340.
(25) Venkatraman, S.; Bogen, S. L.; Arasappan, A.; Bennett, F.; Chen, K.; Jao, E.; Liu, Y. T.; Lovey, R.; Hendrata, S.; Huang, Y. H.; Pan, W. D.; Parekh, T.; Pinto, P.; Popov, V.; Pike, R.; Ruan, S.; Santhanam, B.; Vibulbhan, B.; Wu, W. L.; Yang, W. Y.; Kong, J. S.; Liang, X.; Wong, J.; Liu, R.; Butkiewicz, N.; Chase, R.; Hart, A.; Agrawal, S.; Ingravallo, P.; Pichardo, J.; Kong, R.; Baroudy, B.; Malcolm, B.; Guo, Z. Y.; Prongay, A.; Madison, V.; Broske, L.; Cui, X. M.; Cheng, K. C.; Hsieh, Y. S.; Brisson, J. M.; Prelusky, D.; Korfmacher, W.; White, R.; Bogdanowich-Knipp, S.; Pavlovsky, A.; Bradley, P.; Saksena, A. K.; Ganguly, A.; Piwinski, J.; Girijavallabhan, V.; Njoroge, F. G. Discovery of (1*R*,5*S*)-*N*-[3-amino-1-(cyclobutylmethyl)-2,3-dioxopropyl]-3-[2(*S*)-[[[(1,1-dimethylethyl)amino]carbonyl]amino]-3,3-dimethyl-1-oxobutyl]-6,6-dimethyl-3-azabicyclo[3.1.0]hexan-2(*S*)-carboxamide (SCH 503034), a selective, potent, orally bioavailable hepatitis C virus NS3 protease inhibitor: a potential therapeutic agent for the treatment of hepatitis C infection. *J. Med. Chem.* **2006**, *49*, 6074−6086.
(26) Nilsson, P.; Ofsson, K.; Larhed, M. Microwave-assisted and metal-catalyzed coupling reactions. *Top. Curr. Chem.* **2006**, *266*, 103−144.
(27) Gising, J.; Odell, L. R.; Larhed, M. Microwave-assisted synthesis of small molecules targeting the infectious diseases tuberculosis, HIV/AIDS, malaria and hepatitis C. *Org. Biomol. Chem.* **2012**, *10*, 2713−2729.
(28) Gising, J.; Örtqvist, P.; Sandström, A.; Larhed, M. A straightforward microwave method for rapid synthesis of N-1, C-6 functionalized 3,5-dichloro-2(1*H*)-pyrazinones. *Org. Biomol. Chem.* **2009**, *7*, 2809−2815.
(29) Yin, J. J.; Buchwald, S. L. Pd-catalyzed intermolecular amidation of aryl halides: the discovery that xantphos can be trans-chelating in a palladium complex. *J. Am. Chem. Soc.* **2002**, *124*, 6043−6048.
(30) Pawar, V. G.; De Borggraeve, W. M. 3,5-dihalo-2(1*H*)-pyrazinones: Versatile scaffolds in organic synthesis. *Synthesis (Stuttgart)* **2006**, 2799−2814.
(31) Kaval, N.; Appukkuttan, P.; Van der Eycken, E. The Chemistry of 2-(1*H*)-Pyrazinones in Solution and on Solid Support. In *Microwave-Assisted Synthesis of Heterocycles*; Topics in Heterocyclic Chemistry; Springer-Verlag: Berlin, 2006; *Vol. 1*, pp 267−304.
(32) Olofsson, K.; Nilsson, P.; Larhed, M. Accelerated Chemistry: Microwave, Sonochemical, and Fluorous Phase Techniques. In *Exploiting Chemical Diversity for Drug Discovery*; Bartlett, P. A., Entzeroth, M., Eds.; The Royal Society of Chemistry: Cambridge, UK, 2006; pp 33−53.
(33) Nöteberg, D.; Schaal, W.; Hamelink, E.; Vrang, L.; Larhed, M. High-speed optimization of inhibitors of the malarial proteases plasmepsin I and II. *J. Comb. Chem.* **2003**, *5*, 456−464.
(34) Poliakov, A.; Hubatsch, I.; Shuman, C. F.; Stenberg, G.; Danielson, U. H. Expression and purification of recombinant full-length NS3 protease-helicase from a new variant of Hepatitis C virus. *Protein Express. Purif.* **2002**, *25*, 363−371.
(35) Gulnik, S. V.; Suvorov, L. I.; Liu, B. S.; Yu, B.; Anderson, B.; Mitsuya, H.; Erickson, J. W. Kinetic Characterization and Cross-Resistance Patterns of Hiv-1 Protease Mutants Selected under Drug Pressure. *Biochemistry* **1995**, *34*, 9282−9287.
(36) Danielson, U. H.; Dahl, G.; Sandström, A.; Åkerblom, E. Resistance profiling of hepatitis C virus protease inhibitors using full-length NS3. *Antiviral Ther.* **2007**, *12*, 733−740.
(37) Artursson, P.; Lennernäs, H.; v. d. Waterbeemd, H. High throughput measurement of log *D* and pK_a. In *Methods and Principles in Medicinal Chemistry*; Comer, J. E. A., Ed.; Wiley: Weinheim, Germany, 2003; Vol. *18*, pp 21−45.
(38) Houston, J. B. Utility of In Vitro Drug Metabolism Data in Predicting In Vivo Metabolic Clearance. *Biochem. Pharmacol.* **1994**, *47*, 1469−1479.
(39) Obach, R. S. Prediction of human clearance of twenty-nine drugs from hepatic microsomal intrinsic clearance data: An examination of in vitro half-life approach and nonspecific binding to microsomes. *Drug Metab. Dispos.* **1999**, *27*, 1350−1359.
(40) Hubatsch, I.; Ragnarsson, E. G. E.; Artursson, P. Determination of drug permeability and prediction of drug absorption in Caco-2 monolayers. *Nature Protoc.* **2007**, *2*, 2111−2119.
(41) Galia, E.; Nicolaides, E.; Horter, D.; Lobenberg, R.; Reppas, C.; Dressman, J. B. Evaluation of various dissolution media for predicting in vivo performance of class I and II drugs. *Pharm. Res.* **1998**, *15*, 698−705.
(42) Neuhoff, S.; Artursson, P.; Zamora, I.; Ungell, A. L. Impact of extracellular protein binding on passive and active drug transport across Caco-2 cells. *Pharm. Res.* **2006**, *23*, 350−359.
(43) Bergström, C. A. S.; Strafford, M.; Lazorova, L.; Avdeef, A.; Luthman, K.; Artursson, P. Absorption classification of oral drugs based on molecular surface properties. *J. Med. Chem.* **2003**, *46*, 558−570.
(44) Schiering, N.; D'Arcy, A.; Villard, F.; Simic, O.; Kamke, M.; Monnet, G.; Hassiepen, U.; Svergun, D. I.; Pulfer, R.; Eder, J.; Raman, P.; Bodendorf, U. A macrocyclic HCV NS3/4A protease inhibitor interacts with protease and helicase residues in the complex with its

full-length target. *Proc. Natl. Acad. Sci. U. S. A.* **2011**, *108*, 21052−21056.
(45) Johansson, A.; Poliakov, A.; Åkerblom, E.; Lindeberg, G.; Winiwarter, S.; Samuelsson, B.; Danielson, U. H.; Hallberg, A. Tetrapeptides as Potent Protease Inhibitors of Hepatitis C Virus Full-Length NS3 (Protease-Helicase/NTPase). *Bioorg. Med. Chem.* **2002**, *10*, 3915−3922.
(46) Llinas-Brunet, M.; Bailey, M. D.; Bolger, G.; Brochu, C.; Faucher, A. M.; Ferland, J. M.; Garneau, M.; Ghiro, E.; Gorys, V.; Grand-Maitre, C.; Halmos, T.; Lapeyre-Paquette, N.; Liard, F.; Poirier, M.; Rheaume, M.; Tsantrizos, Y. S.; Lamarre, D. Structure−activity study on a novel series of macrocyclic inhibitors of the hepatitis C virus NS3 protease leading to the discovery of BILN 2061. *J. Med. Chem.* **2004**, *47*, 1605−1608.
(47) Macdonald, S. J. F.; Ritchie, T. J. The impact of aromatic ring count on compound developability—are too many aromatic rings a liability in drug design? *Drug Discovery Today* **2009**, *14*, 1011−1020.
(48) Ritchie, T. J.; Macdonald, S. J. F.; Young, R. J.; Pickett, S. D. The impact of aromatic ring count on compound developability: further insights by examining carbo- and hetero-aromatic and -aliphatic ring types. *Drug Discovery Today* **2011**, *16*, 164−171.
(49) Lovering, F.; Bikker, J.; Humblet, C. Escape from Flatland: Increasing Saturation as an Approach to Improving Clinical Success. *J. Med. Chem.* **2009**, *52*, 6752−6756.
(50) Vermehren, J.; Sarrazin, C. The role of resistance in HCV treatment. *Best Pract. Res. Clin. Gastroenterol.* **2012**, *26*, 487−503.
(51) Pawlotsky, J. M. Treatment Failure and Resistance with Direct-Acting Antiviral Drugs Against Hepatitis C Virus. *Hepatology* **2011**, *53*, 1742−1751.
(52) He, Y.; King, M. S.; Kempf, D. J.; Lu, L.; Ben Lim, H.; Krishnan, P.; Kati, W.; Middleton, T.; Molla, A. Relative replication capacity and selective advantage profiles of protease inhibitor-resistant hepatitis C virus (HCV) NS3 protease mutants in the HCV genotype 1b replicon system. *Antimicrob. Agents Chemother.* **2008**, *52*, 1101−1110.
(53) Courcambeck, J.; Bouzidi, M.; Perbost, R.; Jouirou, B.; Amrani, N.; Cacoub, P.; Pepe, G.; Sabatier, J. M.; Halfon, P. Resistance of hepatitis C virus to NS3-4A protease inhibitors: mechanisms of drug resistance induced by R155Q, A156T, D168A, and D168V mutations. *Antiviral Ther.* **2006**, *11*, 847−855.
(54) Lamarre, D.; Anderson, P. C.; Bailey, M.; Beaulieu, P.; Bolger, G.; Bonneau, P.; Bos, M.; Cameron, D. R.; Cartier, M.; Cordingley, M. G.; Faucher, A. M.; Goudreau, N.; Kawai, S. H.; Kukolj, G.; Lagace, L.; LaPlante, S. R.; Narjes, H.; Poupart, M. A.; Rancourt, J.; Sentjens, R. E.; St George, R.; Simoneau, B.; Steinmann, G.; Thibeault, D.; Tsantrizos, Y. S.; Weldon, S. M.; Yong, C. L.; Llinas-Brunet, M. An NS3 protease inhibitor with antiviral effects in humans infected with hepatitis C virus. *Nature* **2003**, *426*, 186−189.
(55) Lin, C.; Lin, K.; Luong, Y. P.; Rao, B. G.; Wei, Y. Y.; Brennan, D. L.; Fulghum, J. R.; Hsiao, H. M.; Ma, S.; Maxwell, J. P.; Cottrell, K. M.; Perni, R. B.; Gates, C. A.; Kwong, A. D. In vitro resistance studies of hepatitis C virus serine protease inhibitors, VX-950 and BILN 2061—Structural analysis indicates different resistance mechanisms. *J. Biol. Chem.* **2004**, *279*, 17508−17514.